Efficiency study of harmonic generation from solid targets in the strongly relativistic regime

Contact: narenratan@gmail.com

N. Ratan, L. Ceurvorst, M.F. Kasim, J. Sadler and P. Norreys
Department of Physics, University of Oxford, OX1 3PU, United Kingdom

W. Boekee-West, R. Trines and R. Bingham
Central Laser Facility, STFC Rutherford Appleton Laboratory, Didcot, OX11 0QX, United Kingdom

Abstract

In the recent harmonic generation experiments conducted at the University of Michigan [F. Dollar et al., Phys. Rev. Lett. **110**, 175002 (2013)] the harmonics' intensity was found to fall off much faster with harmonic order than in previously observed spectra which confirmed the scaling predicted by Baeva, Gordienko and Pukhov [T. Baeva, S. Gordienko, and A. Pukhov, Phys. Rev. E **74**, 046404 (2006)]. In this paper a comprehensive set of two-dimensional numerical simulations is presented which demonstrate that the efficiency of the harmonic generation process is highly sensitive to very small variations in electron density scalelength.

1 Introduction

Many interesting phenomena have been predicted to occur at laser intensities above $10^{22}\mathrm{W/cm}^2$. These include ion acceleration to GeV energies [1], prolific pair production in QED plasmas [2], fast ignition using radiation pressure acceleration of deuteron beams [3], ultrabright X-ray sources [4], and next generation particle accelerators using laser wakefields [5–8]. The exquisite coherence properties of X-ray harmonics produced from solid targets potentially allow the production of a single coherent attosecond X-ray pulse of ultrabright intensity [9]. Attosecond pulses have already been used to study matter on the timescale of electron motion in atoms and solids [10]. In addition they can be focused to their diffraction limit potentially allowing the electric field in the harmonic focus to reach extraordinary intensities [11].

A simple picture of harmonic generation from solid targets is provided by the oscillating mirror model [12–17]. In this model the thin layer of plasma formed by the incident pulse at the surface of the solid target is considered as a mirror. The incident pulse causes this mirror to oscillate back and forth, and this oscillation causes a sinusoidal Doppler shift of the reflected pulse which gives an oscillating term in its phase. This gives harmonics in its frequency spectrum. This can be demonstrated analytically by writing the phase of the incident pulse as $\omega_0 t$ and the oscillating phase added by the mirror as $a\sin\omega_1 t$, so the phasor of the reflected pulse is $e^{i\omega_0 t + ia\sin\omega_1 t}$. Using the definition of Bessel functions J_n in terms of a generating function [18]

$$e^{\frac{1}{2}z(s-1/s)} = \sum_{n=-\infty}^{+\infty} J_n(z)s^n \tag{1}$$

and taking $z = a$ and $s = \exp(i\omega_1 t)$ gives

$$e^{i\omega_0 t + ia\sin\omega_1 t} = \sum_{n=-\infty}^{+\infty} J_n(a)e^{i(\omega_0 + n\omega_1)t}. \tag{2}$$

An analysis of the action of the incident pulse on the mirror [13] shows that the mirror oscillates at ω_0 and/or $2\omega_0$ depending on the polarization of the incident pulse, so ω_1 is a multiple of ω_0 and the reflected pulse contains frequencies $\omega_0 + n\omega_0$ i.e. harmonics of the incident pulse.

A variety of other models have been proposed to extend our understanding of this process, such as the theory of relativistic spikes [19] and coherent wake emission [20]. Different models are useful descriptions at different intensities. An earlier paper [21] looked at the effect of density scalelength on harmonic generation in an intensity regime where the oscillating mirror model is appropriate; this paper studies the strongly relativistic regime in which the theory of relativistic spikes is more useful. A comprehensive review of harmonic generation from solid targets is given by Teubner and Gibbon [22]. The interested reader is referred to this paper and all the references therein.

The theory of relativistic spikes [19] describes harmonic generation in the strongly relativistic regime. Physically it is based on the fact that in this regime the motion of the electrons in the plasma layer at the surface of the target is such that while the magnitude of their velocity is always close to the speed of light c, the relativistic gamma factor $\gamma_\perp = 1/\sqrt{1 - v_\perp^2/c^2}$ derived from $v_\perp$, the component of their velocity normal to the target surface, undergoes periodic sharp 'spikes' where its value becomes very large. It is during these short relativistic spikes that the electrons produce the harmonics. These relativistic spikes in the motion of the electrons can be understood using the zero vector potential model [23]. Mathematically the theory is based on a rescaling symmetry of the Vlasov equation in the strongly relativistic limit [24, 25], which allows the equation to be written in a dimensionless form depending only on a dimensionless

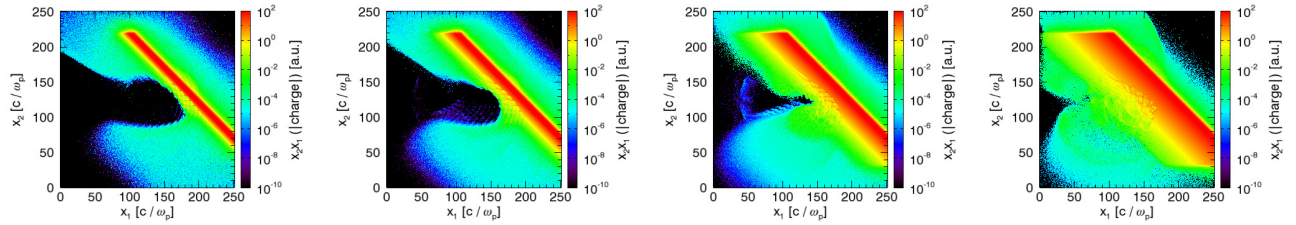

Figure 1: The electron charge density as the incident pulse hits the target for the scalelengths (a) 0.2λ, (b) 0.4λ, (c) 0.75λ and (d) 1.33λ, where λ is the laser wavelength.

parameter $S = n_e/a_0 n_c$ where n_e is the plasma electron density and n_c the critical density associated with the incident laser frequency (the logic here is familiar from the introduction of the Reynolds number in the study of viscous fluids). Together with the use of the 'apparent reflection point' formalism [19], this theory leads to a prediction that the intensity of harmonics produced by a strongly relativistic pulse should fall off with harmonic order n as $n^{-8/3}$. A harmonic spectrum of this form was indeed observed in the experiments of Dromey et al. on the Vulcan Petawatt laser at the Rutherford Appleton Laboratory [26], in which the harmonics were seen to fall off as $n^{-2.5} - n^{-3}$. Up to 3000 harmonic orders have been observed by this team, confirming the harmonic cut-off dependence of the theory of relativistic spikes [27].

In this context, the recent harmonic generation experiments performed at the University of Michigan using the HERCULES laser, in the strongly relativistic regime, are intriguing. They observed a much faster decay of harmonic intensity [28], with $n^{-4.3} - n^{-4.8}$ under optimal conditions and $n^{-5.2} - n^{-10}$ for less ideal conditions. One is led to ask the question: what causes the departure from the previously confirmed scaling in the Michigan experiments? This paper presents a comprehensive set of two-dimensional particle-in-cell simulations answering this question. The simulations show that the harmonic generation process is highly sensitive to very small variations in the electron density scalelength (the 'thickness of the plasma mirror'). Fluctuations in density scalelength lead to a displacement between the focal plane of the laser and the critical density surface. Combined with the tight focusing optics used in the Michigan experiments this leads to a reduction of the laser intensity at reflection.

2 The Michigan experiments

It is worth summarizing some of the interesting features of the Michigan experiments [28] which stimulated the present study. The incident pulse was focused to a spot size of 1.2μm, just one and a half wavelengths of the 800nm radiation produced by the Ti:sapphire system used. The intensity on target was 2×10^{21}W/cm^2, which gives a dimensionless intensity parameter of $a_0 = 31.7$. The layer of plasma used for harmonic generation was formed by a prepulse. The electron density in the plasma layer falls off approximately exponentially with some scalelength. This scalelength was controlled both by varying the strength of the prepulse (by altering the amplified spontaneous emission contrast) and by using solid targets with different damage thresholds. The Michigan team note that the large effect of small fluctuations in prepulse intensity made controlling small variations in the scalelength difficult. The details of the Michigan experiments suggest studying the effects of the electron density scalelength and of the small focal spot on the harmonic generation process. Harmonic generation could also be reduced if magnetic fields generated at the surface of the target caused the incident pulse to become elliptically polarized by the Cotton-Mouton effect [29–32], since the zero vector potential model suggests that for elliptically polarized light relativistic spikes in the electron motion will be reduced.

3 Methods

The simulations were performed using the 2D particle-in-cell code OSIRIS, which ran on the SCARF-LEXICON cluster at the STFC Rutherford Appleton Laboratory. The particle-in-cell algorithm [33] solves for the electromagnetic field and the positions of macroparticles representing electrons and ions. The algorithm uses the macroparticle positions to define charge and current densities which are then used as sources for the electromagnetic field, which in turn acts on the macroparticles via the Lorentz force law. The OSIRIS code uses relativistic equations of motion for the macroparticles.

To find the harmonics in the reflected radiation the 2D discrete Fourier transform of the electric field was used. The values of each component of the electric field were stored on an 8000 × 16000 grid. The discrete Fourier transform of a function f on an $N \times M$ grid is defined on a grid of the same size as follows: writing $f(r, s)$ for the function value at the grid point (r, s) and $F(p, q)$ for the Fourier transform at grid point (p, q),

$$F(p,q) = \frac{1}{NM} \sum_{r=0}^{N-1} \sum_{s=0}^{M-1} f(r,s) e^{-2\pi i (pr/N + qs/M)}. \quad (3)$$

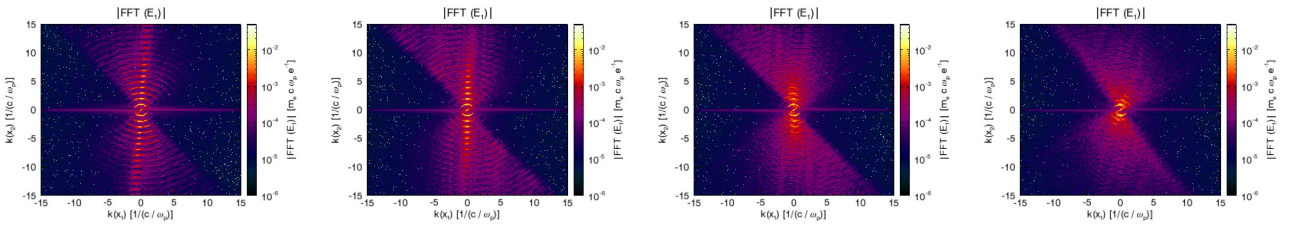

Figure 2: The 2D spectra of the reflected radiation for the scalelengths (a) 0.05λ, (b) 0.2λ, (c) 0.3λ and (d) 0.5λ, where λ is the laser wavelength.

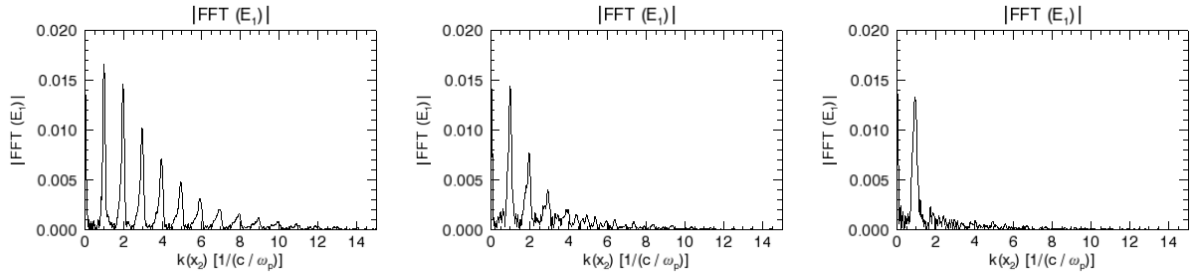

Figure 3: The 1D spectra of the reflected radiation for the scalelengths (a) 0.2λ, (b) 0.3λ and (c) 0.5λ, where λ is the laser wavelength.

Even for real f the Fourier transform is in general complex. The plots of the 2D spectra show the absolute value of the Fourier coefficients (Fig. 2).

The spatial box in our simulations covered a physical area of $32\mu\text{m} \times 64\mu\text{m}$ with a grid of 8000×16000 points. The simulation covered a physical time of 340fs with a timestep of 3.2×10^{-3}fs. The incident laser pulse had a wavelength of 800nm, a length of 53fs, an a_0 of 30, and a spot radius of 0.4μm. Each of the fifteen simulations used 450 CPU hours.

4 Results and Discussion

4.1 Density scalelength

First of all the focus of the incident pulse was kept at a fixed position and the scalelength of the plasma layer was varied to study the effect of the reported scalelength fluctuations.

Figure 1 shows the electron charge density as a function of position as the laser strikes the target in simulations with a range of density scalelengths (a) 0.2λ, (b) 0.4λ, (c) 0.75λ and (d) 1.33λ. In the shortest scalelength case (a) the laser pulse interacts mainly with a thin layer of plasma at the larget surface, while for the longest scalelength (d) the pulse interacts with a large volume of plasma, with no well-defined plasma mirror visible.

Figure 2 shows the 2D discrete Fourier transforms of the x_1-component of the electric field of the reflected pulses for density scalelengths (a) 0.05λ, (b) 0.2λ, (c) 0.3λ and (d) 0.5λ. The presence of well-defined harmonics in the reflected pulse is indicated by rings in the 2D spectra. For a scalelength of 0.05λ many clear harmonics are produced. Increasing the scalelength to 0.2λ gives a broadening of the harmonics. Only the first two harmonics are visible using a scalelength of 0.3λ. For a scalelength of 0.5λ, as well as in the results from even longer scalengths (not shown), there is no harmonic structure at all. The range of scalelengths shown here is less than half a laser wavelength, so the dependence of the harmonic production on scalelength is very sensitive. Figure 3 shows vertical lineouts of the 2D spectra in Fig. 2 which give the spectrum of the radiation propagating in the specular direction. The difference between the spectra for these very similar scalelengths is striking.

4.2 Focus position relative to critical density

A laser beam focused to a small spot will spread rapidly either side of the focus, since the Rayleigh range is proportional to the square of the spot size [34]. This motivated our study of the effect of the laser focus position relative to the critical density (where the pulse is reflected). In these simulations the plasma density scalelength was kept fixed and the position of the laser focus was varied. Figure 4 shows plots of the electric field intensity at the same timestep (around the time of reflection) for the case in which the laser is focused at the critical surface and the case in which it is focused in front of the critical surface. If the focus is in front of the critical surface the pulse has had a chance to diffract con-

siderably by the time it is reflected, and so the pulse has a lower intensity when it is reflected. This means that the intensity at reflection may not be strongly relativistic even if the intensity at focus is, and the $n^{-8/3}$ scaling of harmonic intensity holds only for strongly relativistic intensities.

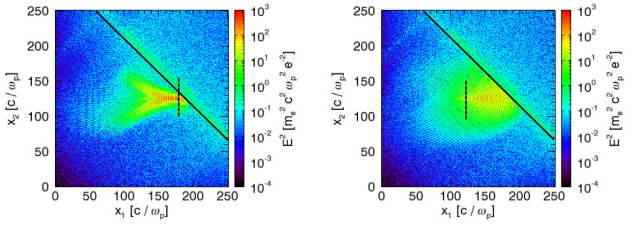

Figure 4: The electric field intensity as the incident pulse hits the target with the focus (a) at the critical density surface or (b) in front of it. The critical density surface is shown by the solid lines, the plane of the focus by the dashed lines.

4.3 Change in polarization due to magnetic fields

A laser pulse with linear polarization can become elliptically polarized as it propagates across a static magnetic field [30–32]. The electric field data from the simulations show no sign of the incident pulse becoming elliptically polarized (this would appear as an oscillating electric field component perpendicular to the initial plane of polarization). The magnetic field data from the simulations do not show significant magnetic fields other than the oscillating fields from the incident and reflected laser pulses.

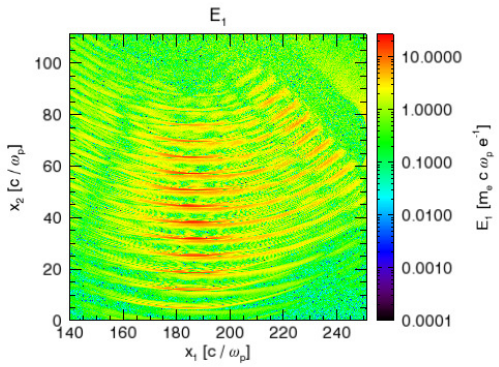

Figure 5: The electric field of the reflected radiation shows intensity maxima and zeroes as a function of angle of propagation.

4.4 Angular distribution of harmonics

The angular distribution of the harmonic radiation displayed an interesting structure (Fig. 5). There are a series of intensity maxima and zeroes in the reflected radiation as a function of angle of propagation with respect to the specular direction. A possible explanation is that during reflection two distinct beams of harmonics appear to be produced, one in the specular direction and one along the target, and the interference of these beams generates the series of intensity peaks in the angular distribution [35]. A simulation with a larger box demonstrated that this angular intensity pattern persists in the harmonic radiation once it has propagated away from the target.

5 Conclusions

Our simulations suggest that the departure of the harmonic spectra from the previously confirmed Baeva-Gordienko-Pukhov scaling is a result of fluctuations in plasma density scalelength and the exact position of the critical surface with respect to that of the laser focus. Small variations in the scalelength can make the difference between strong and essentially zero harmonic production. Using tight focusing optics gives a short Rayleigh range for the beam. This means that if the critical surface is displaced from the focal plane the beam will have diffracted a lot before it reflects, so the intensity at reflection will be lower than the intensity at focus.

While our simulations were directed at understanding the Michigan experiments, the conclusions are relevant to solid-target harmonic generation experiments in general. Control of the density scalelength will be necessary to reduce the currently large shot to shot variations in the harmonics produced in experiments, an important goal if the harmonics are to be used as a practical source. The use of small spot sizes to reach high intensities has the great advantage of accessing the strongly relativistic regime, but has the drawback of a reduced Rayleigh range which increases the sensitivity to variations in scalelength, a factor that must be considered when planning future experiments and interpreting data.

Acknowledgements

This work was supported by EPSRC and STFC. We acknowledge the support of the Computational Science Department at RAL for the use of SCARF-LEXICON, and the UCLA/IST OSIRIS consortium for the use of OSIRIS.

References

[1] T. Esirkepov, M. Borghesi, S. V. Bulanov, G. Mourou, and T. Tajima, Phys. Rev. Lett. **92**, 175003 (2004).

[2] A. R. Bell and J. G. Kirk, Phys. Rev. Lett. **101**, 200403 (2008).

[3] N. Naumova, T. Schlegel, V. T. Tikhonchuk, C. Labaune, I. V. Sokolov, and G. Mourou, Phys. Rev. Lett. **102**, 025002 (2009).

[4] S. Gordienko, A. Pukhov, O. Shorokhov, and T. Baeva, Phys. Rev. Lett. **94**, 103903 (2005).

[5] T. Tajima and J. M. Dawson, Phys. Rev. Lett. **43**, 267 (1979).

[6] S. P. D. Mangles, C. D. Murphy, Z. Najmudin, A. G. R. Thomas, J. L. Collier, A. E. Dangor, E. J. Divall, P. S. Foster, J. G. Gallacher, C. J. Hooker, *et al.*, Nature **431**, 535 (2004).

[7] W. P. Leemans, B. Nagler, A. J. Gonsalves, C. s. Toth, K. Nakamura, C. G. R. Geddes, E. Esarey, C. B. Schroeder, and S. M. Hooker, Nat. Phys. **2**, 696 (2006).

[8] W. P. Leemans, R. Duarte, E. Esarey, S. Fournier, C. G. R. Geddes, D. Lockhart, C. B. Schroeder, C. Toth, J. L. Vay, S. Zimmermann, *et al.*, in *AIP Conf. Proc.*, Vol. 1299 (2010) p. 3.

[9] T. Baeva, S. Gordienko, and A. Pukhov, Phys. Rev. E **74**, 065401 (2006).

[10] F. Krausz and M. Ivanov, Rev. Mod. Phys. **81**, 163 (2009).

[11] B. Dromey, D. Adams, R. Hörlein, Y. Nomura, S. G. Rykovanov, D. C. Carroll, P. S. Foster, S. Kar, K. Markey, P. McKenna, *et al.*, Nat. Phys. **5**, 146 (2009).

[12] R. Lichters, J. Meyer-ter Vehn, and A. Pukhov, Phys. Plasmas **3**, 3425 (1996).

[13] D. Von der Linde and K. Rzazewski, Appl. Phys. B **63**, 499 (1996).

[14] S. V. Bulanov, N. M. Naumova, and F. Pegoraro, Phys. Plasmas **1**, 745 (1994).

[15] S. C. Wilks, W. L. Kruer, and W. B. Mori, IEEE T. Plasma Sci. **21**, 120 (1993).

[16] P. A. Norreys, M. Zepf, S. Moustaizis, A. P. Fews, J. Zhang, P. Lee, M. Bakarezos, C. N. Danson, A. Dyson, P. Gibbon, *et al.*, Phys. Rev. Lett. **76**, 1832 (1996).

[17] D. von der Linde, T. Engers, G. Jenke, P. Agostini, G. Grillon, E. Nibbering, A. Mysyrowicz, and A. Antonetti, "bibfield journal "bibinfo journal Phys. Rev. A" "textbf "bibinfo volume 52," "bibinfo pages R25 ("bibinfo year 1995).

[18] E. T. Whittaker and G. N. Watson, *A Course of Modern Analysis* (Cambridge University Press, 1927).

[19] T. Baeva, *High Harmonic Generation from Relativistic Plasmas: Relativistic Similarity, Subattosecond Pulses, and Coherent X-rays* (VDM Verlag, 2008).

[20] C. Thaury and F. Quéré, J. Phys. B **43**, 213001 (2010).

[21] M. Zepf, G. D. Tsakiris, G. Pretzler, I. Watts, D. M. Chambers, P. A. Norreys, U. Andiel, A. E. Dangor, K. Eidmann, C. Gahn, *et al.*, Phys. Rev. E **58**, R5253 (1998).

[22] U. Teubner and P. Gibbon, Rev. Mod. Phys **81**, 445 (2009).

[23] T. Baeva, S. Gordienko, A. P. L. Robinson, and P. A. Norreys, Phys. Plasmas **18**, 056702 (2011).

[24] S. Gordienko and A. Pukhov, Phys. Plasmas **12**, 043109 (2005).

[25] S. Gordienko, A. Pukhov, O. Shorokhov, and T. Baeva, arXiv preprint , physics/0406019 (2004).

[26] B. Dromey, M. Zepf, A. Gopal, K. Lancaster, M. S. Wei, K. Krushelnick, M. Tatarakis, N. Vakakis, S. Moustaizis, R. Kodama, *et al.*, Nat. Phys. **2**, 456 (2006).

[27] B. Dromey, S. Kar, C. Bellei, D. C. Carroll, R. J. Clarke, J. S. Green, S. Kneip, K. Markey, S. R. Nagel, P. T. Simpson, *et al.*, Phys. Rev. Lett. **99**, 085001 (2007).

[28] F. Dollar, P. Cummings, V. Chvykov, L. Willingale, M. Vargas, V. Yanovsky, C. Zulick, A. Maksimchuk, A. G. R. Thomas, and K. Krushelnick, Phys. Rev. Lett. **110**, 175002 (2013).

[29] R. N. Sudan, Phys. Rev. Lett. **70**, 3075 (1993).

[30] S. E. Segre, Plasma Phys. Contr. F. **41**, R57 (1999).

[31] M. Tatarakis, I. Watts, F. N. Beg, E. L. Clark, A. E. Dangor, A. Gopal, M. G. Haines, P. A. Norreys, U. Wagner, M.-S. Wei, *et al.*, Nature **415**, 280 (2002).

[32] U. Wagner, M. Tatarakis, A. Gopal, F. N. Beg, E. L. Clark, A. E. Dangor, R. G. Evans, M. G. Haines, S. P. D. Mangles, P. A. Norreys, *et al.*, Phys. Rev. E **70**, 026401 (2004).

[33] C. K. Birdsall and A. B. Langdon, *Plasma Physics via Computer Simulation* (CRC Press, 2004).

[34] A. E. Siegman, *Lasers* (University Science Books, 1986).

[35] D. an der Brügge, N. Kumar, A. Pukhov, and C. Rödel, Phys. Rev. Lett. **108**, 125002 (2012).